Original Research Article

EXPERIMENTAL AND NUMERICAL STUDY ON STRENGTHENING OF R.C SLABS AT TENSION SIDE USING LOWER CONCRETE LAYER REINFORCED BY FRP ELEMENTS.

.

ABSTRACT

Aims: Study the strengthening of reinforced concrete slabs at tension side using lower concrete layer reinforced by FRP bars. The proposed layer improves strongly the flexural strength and the rigidity of R.C slabs, moreover, FRP elements are noncorrosive in contrast with the traditional strengthening layers reinforced by steel bars.
Study design: Parametric study is carried out by varying the material type, thickness of strengthening layer, spacing between strengthening layer reinforcement bars, cross sectional area of this reinforcement and the type of the strengthening reinforcement.
Methodology: This study presents the efficiency of adding lower concrete layer reinforced by different materials to increase the flexural strength for two-way R.C slabs. Eleven half-scale two-way R.C slab specimens were prepared and tested under four point bending. One of these slabs was unstrengthened and considered as a control specimen. The other specimens were strengthened by using different lower concrete layers reinforced mainly by fiber reinforced polymer (FRP) bars. The parameters of this study included the material type (reinforcement steel, glass fiber and carbon fiber), the thickness of strengthening layer (30 & 50 mm), spacing between strengthening layer reinforcement bars (100 & 200 mm), cross sectional area of this reinforcement (A & 2A) and the type of the strengthening reinforcement (FRP bars & FRP strips).
Results: The experimental results included cracking load, ultimate load, load-deflection relationships, relative ductility, and flexural stiffness.
Conclusion: The experimental results showed an improvement in the flexural behavior of the strengthened specimens compared to control specimen. The flexural strength of the different strengthened specimens increased by 37% to 112% compared to the control specimen. Moreover, a finite element models were developed by ANSYS (version 15) to simulate all the tested specimens. The results calculated based on FEM models were in good agreement with the corresponding experimental ones. However, the calculated ultimate loads were slightly higher than the experimental ultimate loads up to 12%.

Keywords: Two-way R.C slabs, Flexure Failure, strengthening, Fiber Reinforced Polymer and finite element analysis.

1. INTRODUCTION

Strengthening and repairing of reinforced concrete structures are frequently required due to inadequate maintenance, excessive loading, change in use or in code of practice and exposure to adverse environmental condition [1]. Several strengthening techniques have been developed by different traditional techniques including steel plate bonding, external prestressing and reinforced concrete jacting [2,3,4,5]. Reinforced concrete solid slabs are used in floors and as decks of bridges. Slabs may span in one direction or in two directions depending on the slab dimension and the surrounding supporting elements. Different strengthening techniques have been developed so that its serviceability and strength can be restored. Also, the strengthening of the structure should be done taking into consideration the durability aspect. Nowadays, various strengthening techniques are available. However, the selection of the proper technique depends on many factors; such as the deficiency aspect of RC slabs, the cost of the proposed technique, the conditions to which the RC slabs are exposed and the availability of the selected technique [1]. Recently, using FRP materials to strengthen the different RC elements are gaining popularity due to their superior properties which may exceed the steel. The FRP elements have high strength to weight ratio, ease of application, non-magnetic and non-corrosive. Different FRP systems can be applied to strengthen the RC slabs, these systems include externally bonded FRP strips, near surface mounted elements and external post tension tendon [6,7,8,9,10]. This study concerns with evaluating the using of RC lower layer reinforced by FRP bars as a strengthening system for two-way RC slabs.

2. EXPERIMENTAL INVESTIGATION

Eleven specimens were cast and tested to investigate strengthening of two-way R.C slabs using lower concrete layer reinforced by FRP bars. The tested specimens in this study were half-scale models of a typical prototype solid slab structure with equal spans of 180 cm in both directions. All the tested specimens were two-way simply supported slabs.

2.1 Details of test specimens

All the R.C specimens have square shape of 2000×2000 mm in plan. The thickness of the control specimen and the rest of specimens prior to strengthening is 70 mm. The tested specimens were designed to be simply supported along the four edges using line support on each side. Normal mild steel bars of 8 mm diameters with 200 mm spacing in each direction were used as main reinforcement. Full details of the control specimen and the other specimen prior to strengthening, are shown in Fig. 1. The specimens are divided into six groups in addition to the control specimen, as shown in Table 1.

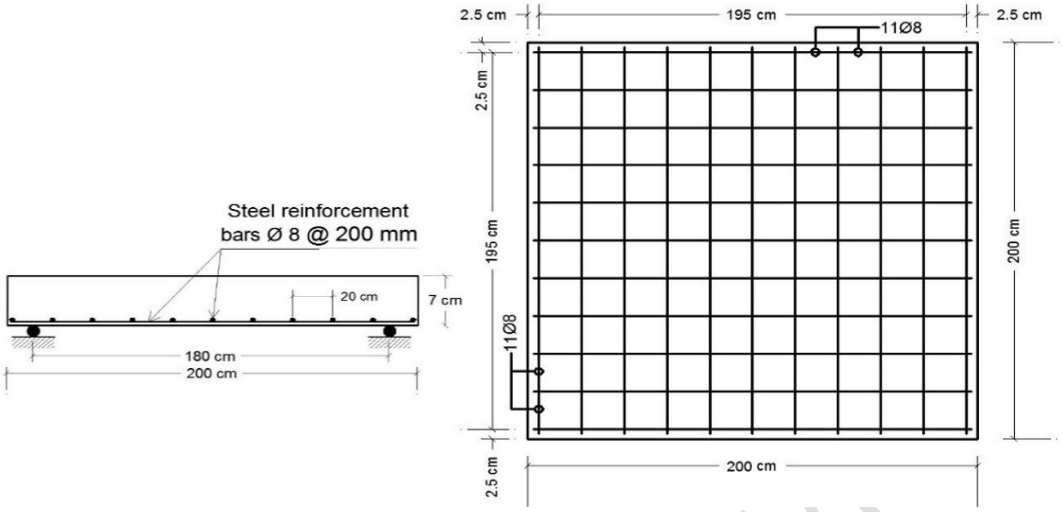

Fig. 1. Dimensions and reinforcement details of the control specimen and the other specimens prior to strengthening.

Table 1. The experimental test program.

Group	Specimen code	Specimen status	Strengthening layer			
			Reinforcement	Layer thickness (mm)	Bars/sheet spacing (mm)	**Area of reinforcement bars/sheets (mm^2)
Control	C	control	---	---	---	---
First group	S-3-20-As	Strengthening	Steel bars	30	200	50.3
Second group	C-3-10-Ac/2		CFRP bars	30	100	28.3
	C-3-20-Ac				200	50.3
Third group	G-3-10-Ag/2		GFRP bars	30	100	28.3
	G-3-20-Ag				200	50.3
Fourth group	G-5-10-Ag/2		GFRP bars	50	100	28.3
	G-5-20-Ag				200	50.3
Fifth group	G-3-10-Ag		GFRP bars	30	100	50.3
	G-5-10-Ag			50	100	50.3
Sixth group	GS-1.5-20-Ag		GFRP sheets*	15	200	70.0

* Externally bonded

** The area of steel or FRP cross-sectional

2.2 Preparation of test specimens

The moulds were prepared and assembled in order to fulfill the required dimensions of the specimens. After the steel reinforcement were installed, concrete mix was placed then the concrete was vibrated mechanically and the concrete surface was finished. After curing

period, the specimens were left in the lab atmosphere until strengthening date. Ten specimens were strengthened, nine specimens were strengthened by FRP element and one specimen by steel bars. Two strengthening techniques were used. For first technique; specimen surface was notched to achieve rough surface using an angle grinder. 10 mm diameter holes were drilled at the arranged positions of anchors (each 400 mm in both directions with staggered shape). Anchors were fixed using sikadur 31 CF and the reinforcement bars were installed to the specimen. Surface of specimens was sprinkled by Addibond 65 to improve the bond between original specimen and strengthening layer, then concrete layer was placed and finished. For second technique; Specimen surface was removed from any unevenness and Sikadur 330 epoxy resin was applied at the areas where GFRP strips were installed in the two directions by using special roller. Figs. (2, 3 & 4) illustrates details of strengthening systems.

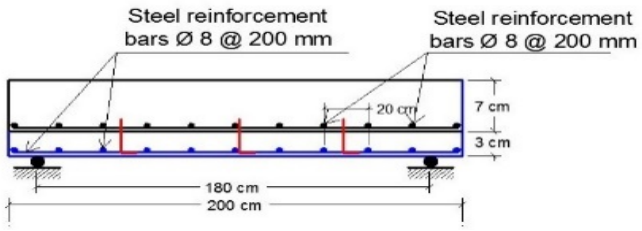

Fig. 2. Adding lower concrete layer reinforced by steel reinforcement mesh

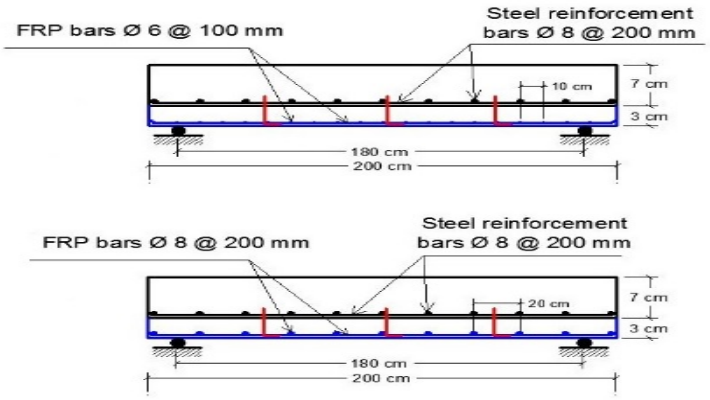

Fig. 3. Adding lower concrete layer reinforced by FRP bars

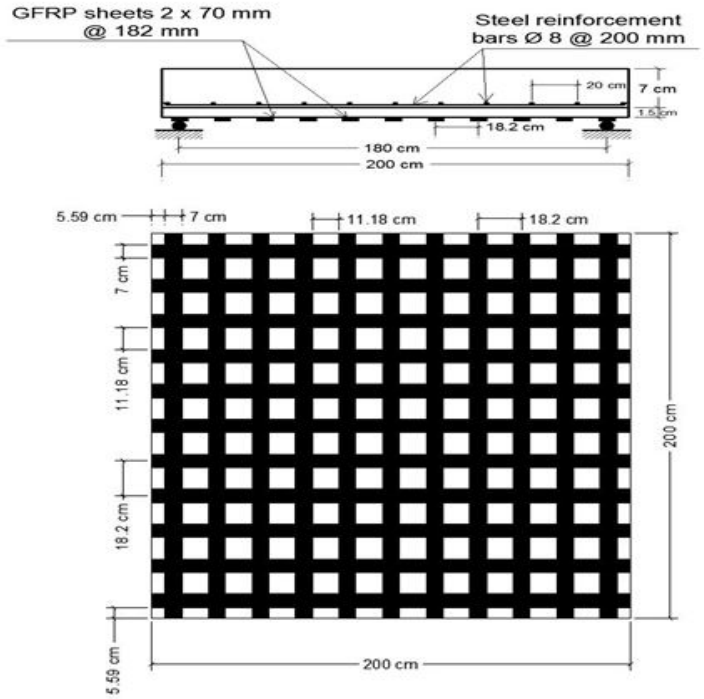

Fig. 4. Adding lower concrete layer reinforced externally by bonded GFRP strips

3. MATERIAL PROPERTIES.

3.1 Concrete

Suitable mix of 305 kg/cm^2 cubic compressive strength after 28 days was used. The constituents of concrete mix and its proportions are presented in Table 2.

Table 2. The constituents of concrete mix.

Cement (Kg/m^3)	Crushed dolomite (Kg/m^3)	Sand (Kg/m^3)	Water (Liter/m^3)
350	1260	630	175

3.2 FRP

CFRP and GFRP bars were locally fabricated using pultrusion process with polyester polymer, then their surfaces were coated by sand layer to improve its bond. The Mechanical properties of FRP bars are given in Table 3. GFRP sheets are, also, locally fabricated. The number of strands in the GFRP strips is the same as in the GFRP bars. The Mechanical properties of GFRP sheets are given in Table 4.

3.3 steel bars

8 mm diameter of normal mild steel bars are used to reinforce the tested specimens and, also, were used as reinforcement for strengthening layer for specimen (S-3-20-As).

Table 3. Dimensional and mechanical properties of FRP bars

Property	GFRP bars		CFRP bars	
Diameter of bars	8 mm	6 mm	8 mm	6 mm
Area of bars	50 mm^2	28.3 mm^2	50 mm^2	28.3 mm^2
Area of fibers	14.55 mm^2	7.75 mm^2	12.8 mm^2	6.4 mm^2
Fiber ratio by area	30%	28%	26%	23%
Tensile strength of fibers	13700 kg/cm^2		14000 kg/cm^2	
Modulas of elasticity of fibers	900000 kg/cm^2		2100000 kg/cm^2	
Strain at failure	15000 x 10^{-6}		6600 x 10^{-6}	

Table 4. Dimensional and mechanical properties of FRP sheets

Property	GFRP
Fabric design thickness	1 mm
Fabric width	7 cm
Tensile strength	22500 kg/cm^2
Modulus of elasticity	760000 kg/cm^2
Strain at failure	2.80%

4. TEST PROCEDURE

The loading system consisted of rigid system of reaction frame, 100 ton capacity, and hydraulic jack, 100 ton capacity, connected to electrical pump. The specimens were tested under vertical concentrated load which is distributed to four equal point concentrated loads acting on the slab upper surface by means of rigid steel frame, as shown in Fig. 5. The specimens were simply supported on line supports at the four sides over a clear span of 1800 mm. Vertical deflection, first cracking load and ultimate failure load, were recorded. Five linear variable differential transducers (LVDTs) mounted at the bottom soffit of the specimen for measuring deflections at bottom face (tension side), as shown in Fig. 6. Cracks propagation was monitored after each load increment up to failure.

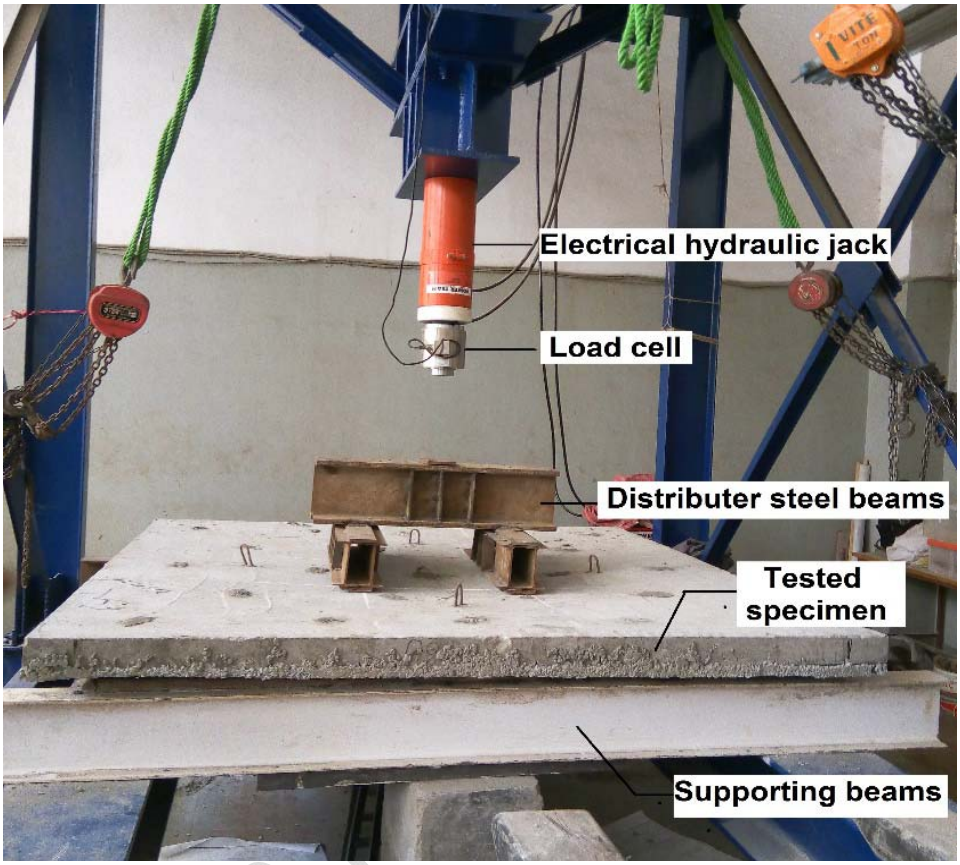

Fig. 5. Test set up

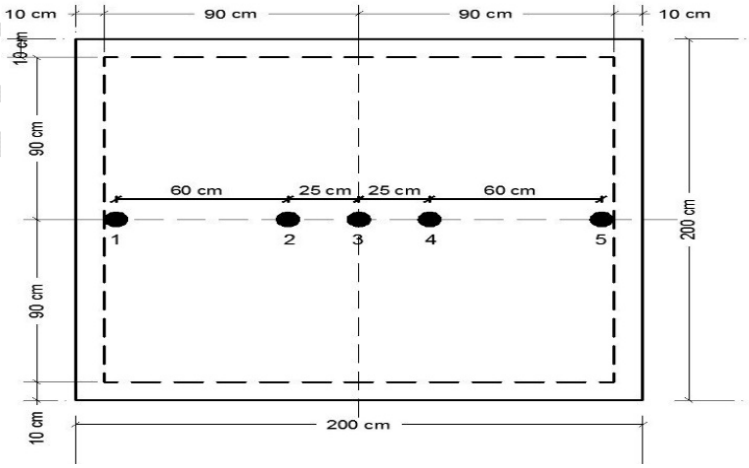

Fig. 6. LVDT locations (bottom side).

5. RESULTS AND DISCUSSION

For the all tested specimens, the relationship between the central deflection at mid-point (point 3) and the applied load was plotted and the crack propagation was monitored with load increasing till failure, Also, the cracking load and ultimate load were recorded. Comparisons between the results of different specimens were carried out to reveal the effect of the parameters considered in this study.

5.1 Load-deflection relationships

All the strengthening systems used in this study led to a significant increase in the strength and the rigidity of the strengthened specimens in comparison with the control specimen. At the same loading level, lower deflection values were recorded for strengthened specimens, either with steel reinforcement, GFRP or CFRP bars, in comparison with the control specimen, as shown in Figs. (7 to 16).

5.1.1 Effect of strengthening layer thickness

The used layers thickness are 30 & 50 mm, respectively. The effect of this parameter could be observed by studying the behavior of specimens G-3-10-Ag/2 & G-5-10-Ag/2, specimens G-3-20-Ag & G-5-20-Ag and specimens G-3-10-Ag & G-5-10-Ag, as shown in Figs. (7, 8 & 9).

As expected, adding the strengthening layer led to improve the flexural behavior. The ultimate load was higher than that of control specimen by 76% and 112% for strengthening layer with thickness 30 mm and 50 mm, respectively. Also, the deflection was reduced by 83.8% and 97.5%, respectively at ultimate recorded load of control specimen.

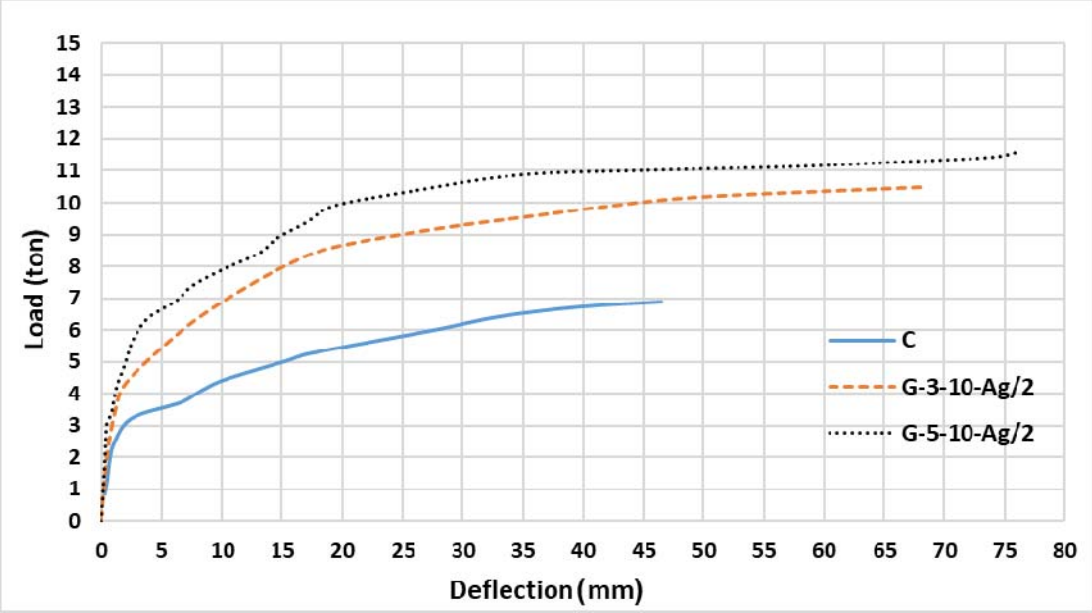

Fig. 7. Comparison between Load-Central deflection relationships of the specimens (G-3-10-Ag/2), (G-5-10-Ag/2), and (C).

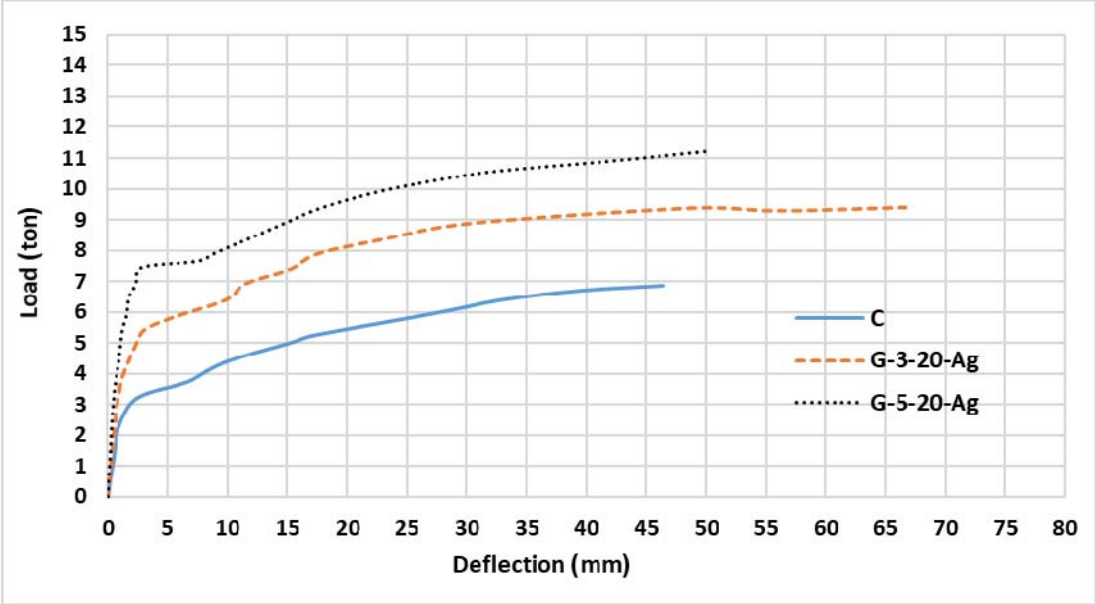

Fig. 8. Comparison between Load-Central deflection relationships of the specimens (G-3-20-Ag), (G-5-20-Ag), and (C).

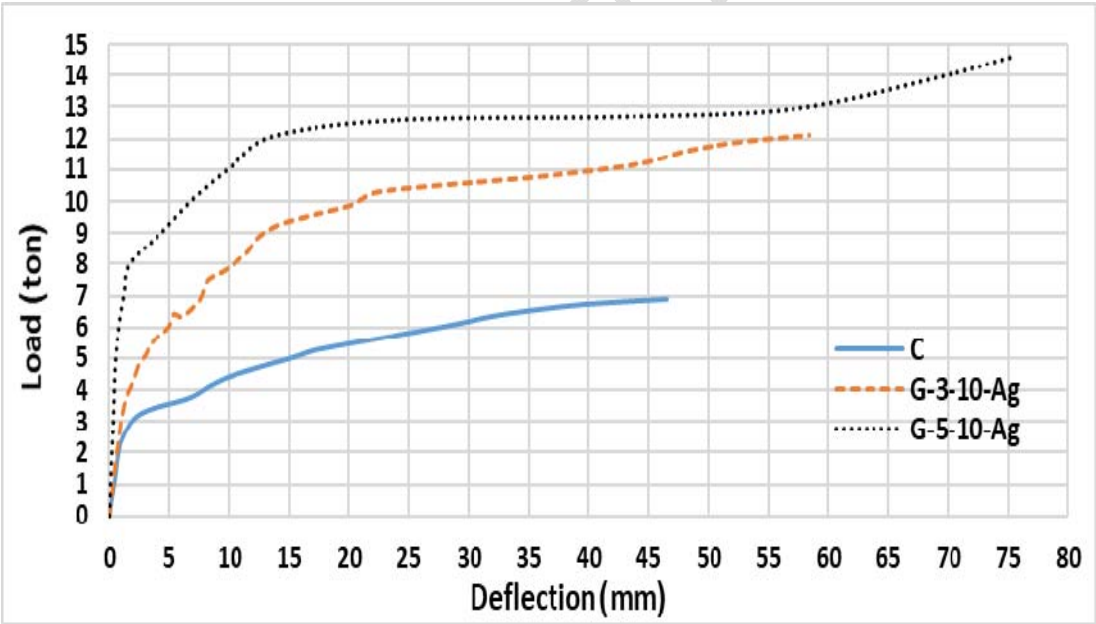

Fig. 9. Comparison between Load-Central deflection relationships of the specimens (G-3-10-Ag), (G-5-10-Ag), and (C).

5.1.2 Effect of strengthening material type

The effect of this parameter could be observed by studying the behavior of specimens S-3-20-As, C-3-20-Ac & G-3-20-Ag, as shown in Fig. 10, which correspond to three types of strengthening materials: steel reinforcement bars, CFRP bars, and GFRP bars.

All the materials used in strengthening led to improve the flexural behavior, where the ultimate load was increased and the deflection at the same loading values was decreased. CFRP bars were the best material, the ultimate load was increased by 68%. However, GFRP bars and steel bars have close ultimate load of 137 % and 138%, respectively of the corresponding control specimen value. The deflection at ultimate load of control specimen was reduced by 80.6%, 75.3% and 92% for specimens strengthened by CFRP, GFRP and steel bars, respectively.

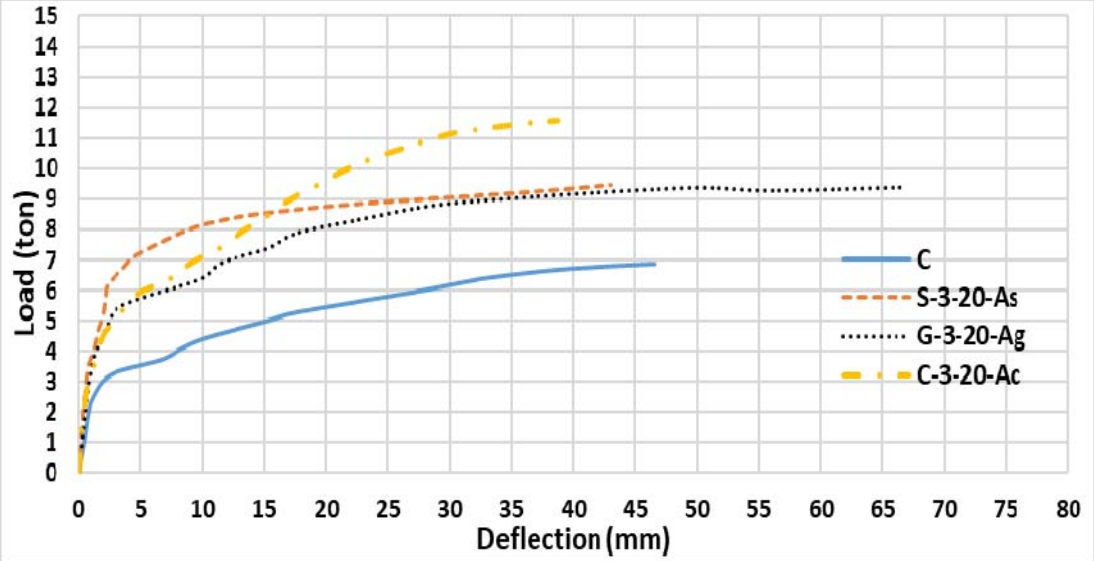

Fig. 10. Comparison between Load-Central deflection relationships of the specimens (S-3-20-As), (C-3-20-Ac), (G-3-20-Ag), and (C).

5.1.3 Effect of spacing between reinforcement bars

The effect of this parameter could be observed by studying the behavior of three specimen groups (G-3-10-Ag/2 & G-3-20-Ag, G-5-10-Ag/2 & G-5-20-Ag and C-3-10-Ac/2 & C-3-20-Ac), as shown in Figs. (11, 12 & 13). The used spacing are 100 & 200 mm, respectively.

Reducing the spacing between bars with keeping the same cross-sectional area led to increase the ultimate load by 53%, 69% and 95% for the three studied groups, respectively compared to that recorded for the control specimen.

The effect of this parameter was more pronounced for CFRP, not only on the ultimate load but also on the deflection reduction, which decreased at maximum recorded load of control specimen by 93.1% when the spacing was reduced from 200 mm to 100 mm.

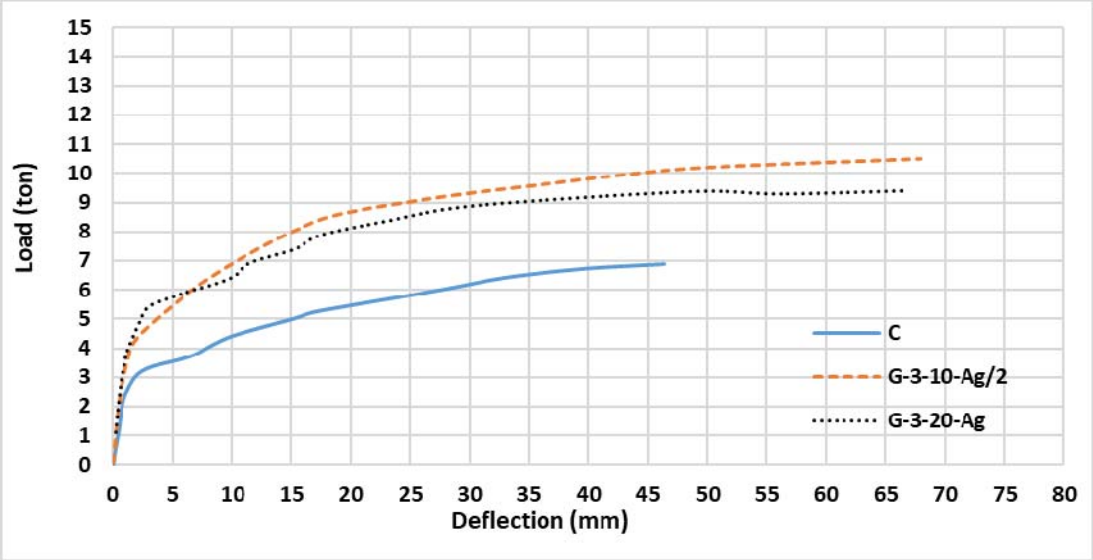

Fig. 11. Comparison between Load-Central deflection relationships of the specimens (G-3-10-Ag/2), (G-3-20-Ag), and (C).

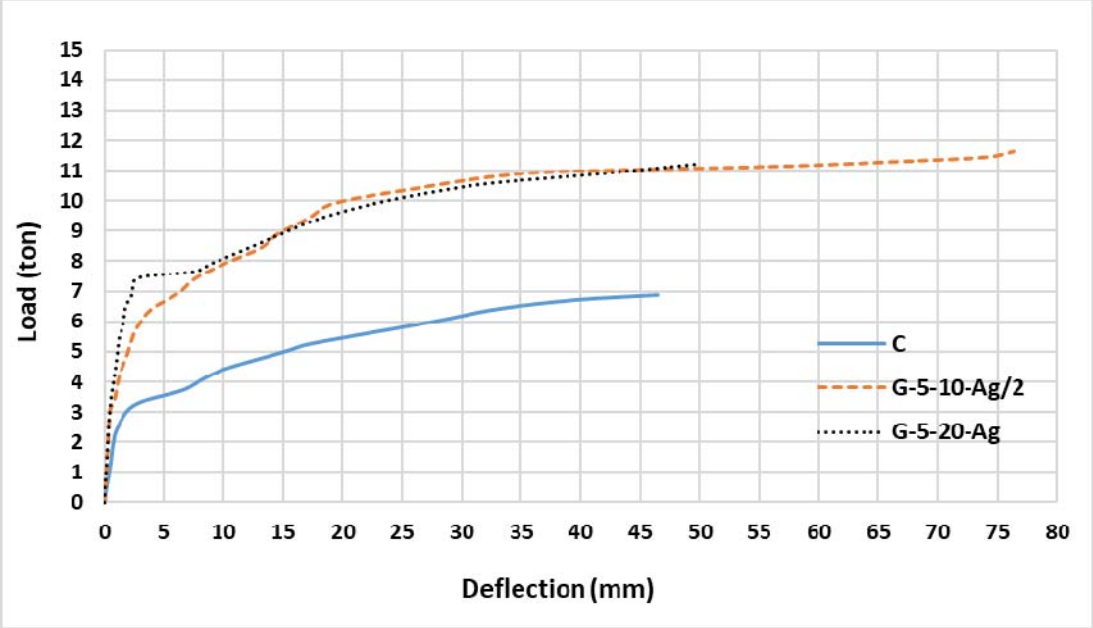

Fig. 12. Comparison between Load-Central deflection relationships of the specimens (G-5-10-Ag/2), (G-5-20-Ag), and (C).

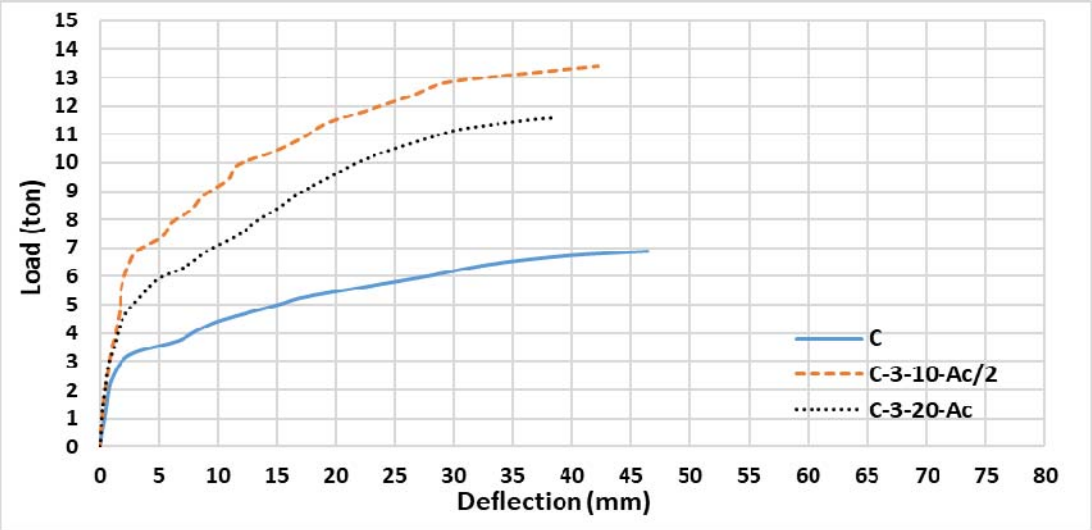

Fig. 13. Comparison between Load-Central deflection relationships of the specimens (C-3-10-Ac/2), (C-3-20-Ac) and (C).

5.1.4 Effect of x-sectional area of reinforcement bars

The effect of this parameter could be observed by studying the behavior of specimens (G-3-10-Ag/2 & G-3-10-Ag and specimens G-5-10-Ag/2 & G-5-10-Ag), as shown in Figs. (14 & 15). For the used areas A & 2A mm, respectively.

As expected, doubling the x-sectional area of bars led to increase the ultimate load by 76% and 112% for specimens strengthening by adding RC layer reinforced by GFRP bars with thickness 30 mm and 50 mm, respectively, also, the deflection at maximum recorded load of control specimen was reduced by 83.8% and 97.5%, respectively in compared with control specimen.

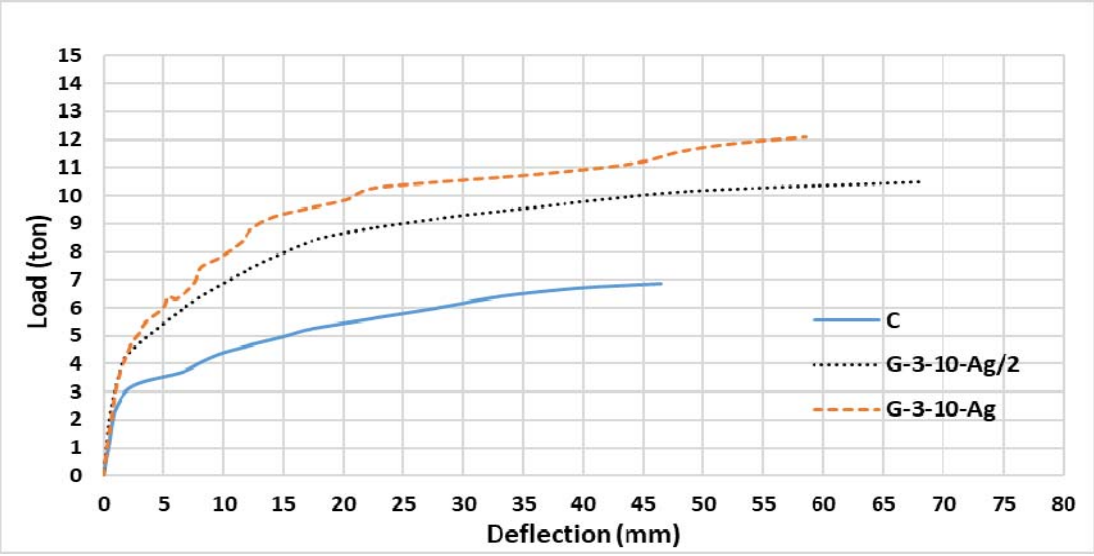

Fig. 14. Comparison between Load-Central deflection relationships of the specimens (G-3-10-Ag/2), (G-3-10-Ag), and (C).

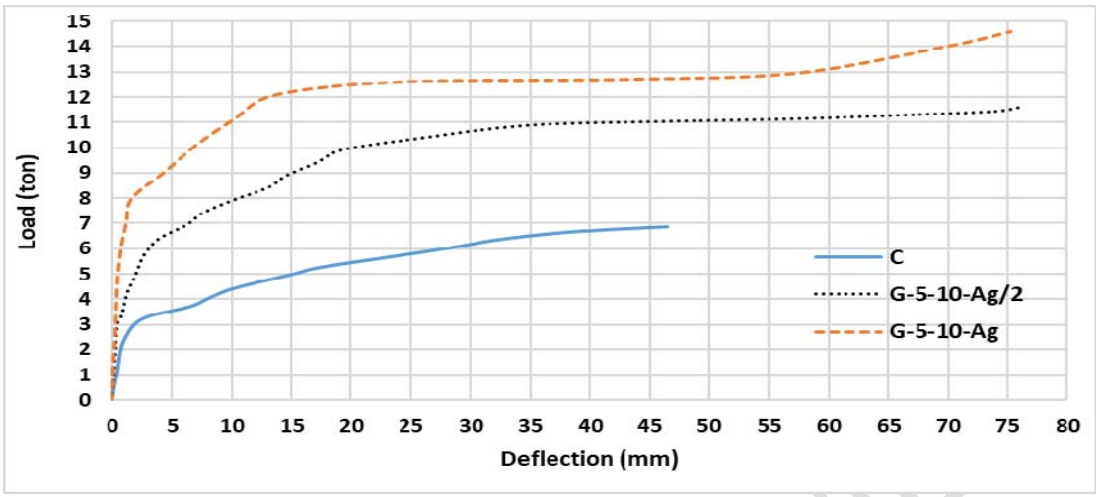

Fig. 15. Comparison between Load-Central deflection relationships of the (G-5-10-Ag/2), (G-5-10-Ag), and (C).

5.1.5 Effect of strengthening method

The effect of this parameter could be observed by studying the behavior of specimens (G-3-20-Ag & GS-1.5-20-Ag), as shown in Fig. 16, which correspond to two types of strengthening methods. The first type was adding 30 mm lower concrete layer reinforced by GFRP bars mesh, and the second was adding 15 mm lower concrete layer reinforced by externally bonded GFRP sheets.

The two strengthening techniques led to increase the ultimate load by 53% and 71% for the first and second technique, respectively compared to the control specimen, also, the deflection at maximum recorded load of control specimen was reduced by 75.3% and 75.9%, respectively in compared with control specimen.

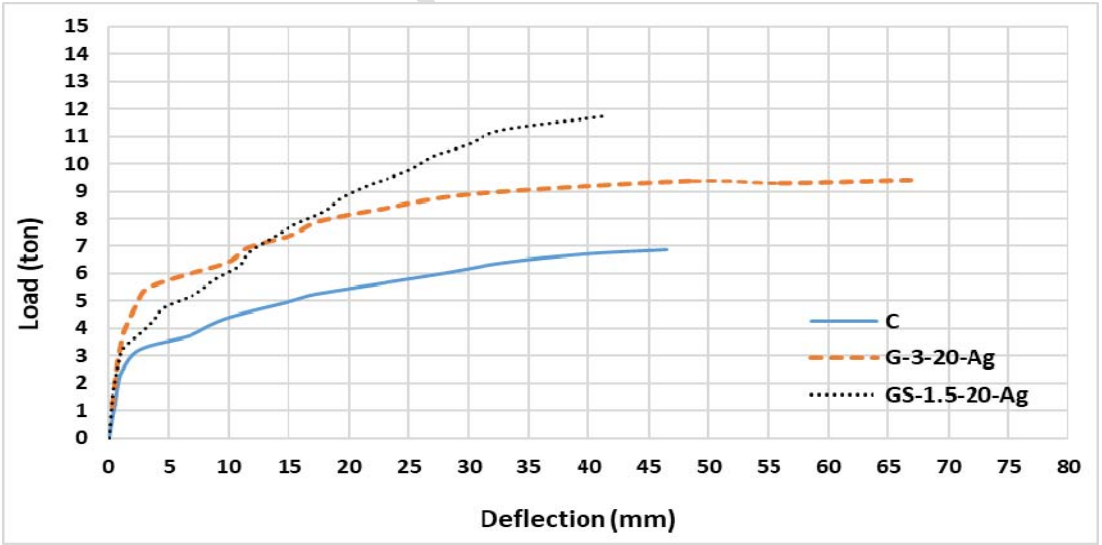

Fig. 16. Comparison between Load-Central deflection relationships of the (G-3-20-Ag), (GS-1.5-20-Ag), and (C).

5.2 Cracking load and ultimate load.

Table. 5 presents the deflection and load values at first cracking and at failure, and also the ductility and the stiffness indices, for all the tested specimens. The specimen (G-5-10-Ag), had the highest ultimate load, higher than that of control specimen by 112%. This was expected because the former specimen has the more effective strengthening system with a lower concrete layer of 50 mm thickness (the biggest thickness) reinforced by GFRP bars of double cross sectional area. The specimen (C-3-10-Ac/2) had the highest ultimate load value, compared to all the specimens of lower layer of 30 mm thickness, the ultimate load of this specimen was higher than that of control specimen by 95%. The high tensile strength of carbon fiber and the small spacing between the CFRP bars (high surface area) may explain the efficient strengthening system of specimen (C-3-10-Ac/2). Fig. 17 shows cracking load and ultimate load values for all specimens.

Table. 5. Main results of the tested specimens.

Specimen code	1st cracking		Ultimate		P_{ult} (specimen) / P_{ult} (control)	Ductility Δ_{ul} / Δ_{cr}	$K_i = P_{cr}/\Delta_{cr}$ (t/mm)	$K_u = \frac{P_{ul}-P_{cr}}{\Delta_{ul}-\Delta_{cr}}$ (t/mm)	Stiffness Degradation $\frac{(K_i-K_u)x100}{K_i}$
	Load (ton)	Δ_{cr} def. (mm)	Load (ton)	Δ_{ul} ult. (mm)					
C	2.00	0.79	6.88	46.50	1.00	58.86	2.53	0.11	95.79
S-3-20-As	4.00	1.23	9.46	43.10	1.38	34.92	3.24	0.13	95.98
C-3-10-Ac/2	5.00	1.75	13.40	42.17	1.95	24.06	2.85	0.21	92.71
C-3-20-Ac	4.00	1.50	11.58	38.78	1.68	25.85	2.67	0.20	92.38
G-3-10-Ag/2	4.50	2.50	10.50	68.00	1.53	27.20	1.80	0.09	94.91
G-3-20-Ag	4.00	1.18	9.40	66.90	1.37	56.79	3.40	0.08	97.58
G-5-10-Ag/2	5.10	2.00	11.64	76.35	1.69	38.17	2.55	0.09	96.55
G-5-20-Ag	4.00	0.74	11.23	50.00	1.63	67.27	5.38	0.15	97.27
G-3-10-Ag	3.00	0.98	12.10	58.46	1.76	59.55	3.06	0.16	94.82
G-5-10-Ag	8.00	1.67	14.59	75.25	2.12	45.09	4.79	0.09	98.13
GS-1.5-20-Ag	5.50	7.10	11.74	41.16	1.71	5.14	0.69	0.19	72.62

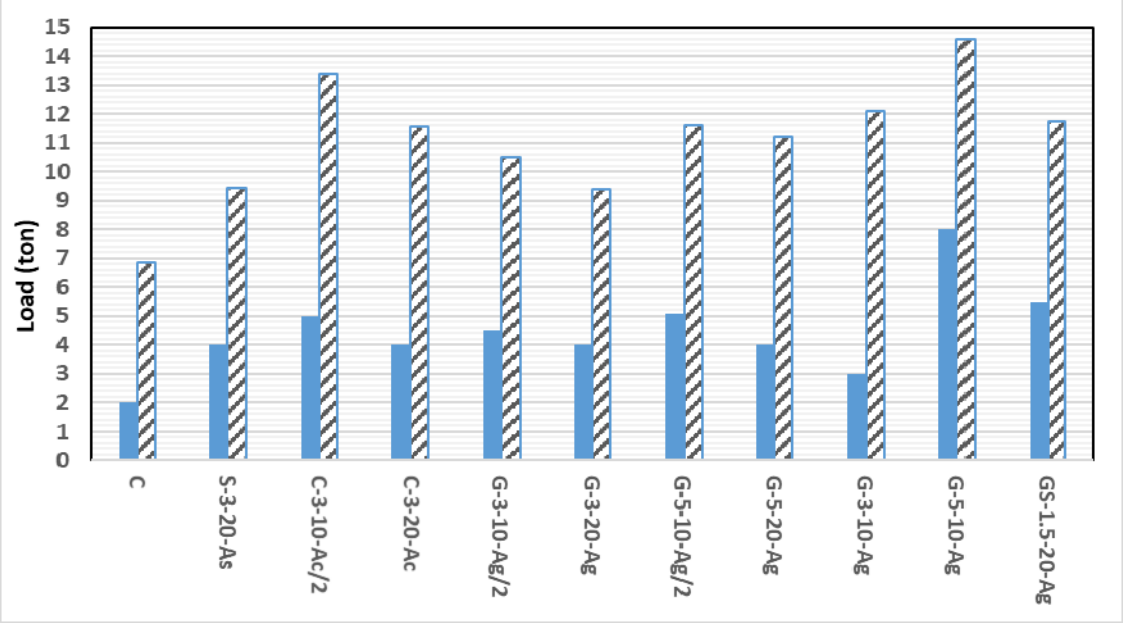

Fig. 17. Cracking and ultimate load for all specimens

5.3 Ductility

Ductility means the ability of a member to undergo inelastic deformations beyond the yield deformation without any considerable loss of load bearing capacity. The ductility of the specimens was considered as the ratio of the deflection at ultimate load to the deflection at first crack load as shown in Table. 5. Generally, specimens strengthened by adding lower concrete layer reinforced by GFRP bars are better than specimens strengthened by adding lower concrete layer reinforced by CFRP bars due to lower modulas of elasticity for GFRP than CFRP, but specimen strengthened by externally bonded GFRP sheets had the less ductility at all due to the high ability of sheets to debond.

5.4 Stiffness

The un-cracked stiffness Ki and the ultimate stiffness Ku were obtained from the load-deflection values of the tested specimens, as presented in Table. 5. It shows that the un-cracked stiffness (Ki) is almost, increased for the majority of the tested specimens. Adding lower concrete layer reinforced by reinforcement steel, CFRP& GFRP bars mesh led to increase Ki while adding lower concrete layer reinforced by externally bonded GFRP sheets led to decrease Ki.

5.5 Cracking behavior and mode of failure.

All the tested specimens were loaded until failed due to flexure. For all specimens, the first crack was recorded, cracks propagation was monitored, and the plane of failure was observed to investigate the cracking and failure behavior. Two modes of failure are expected, the first was flexure failure of the strengthening slab as a one units, while the second type was the debonding between the strengthening layer and the original slab. All specimens were failed by flexure failure with partial debonding between the strengthening

layer and the original slab. Table. 5. shows the load value corresponding to cracking initiation (P_{cr}). Cracks began firstly at the slab tension side under the four point load forming square lines. As the applied loads increase the number and width of the cracks increase then new cracks develop and begin to propagate towards the slab edges in diagonal directions towards the slab corners. The failure surface of the tested specimens was carefully recorded. Strengthening systems led to an increase of the first crack load and, also, its rates to the ultimate load of the tested specimens. A typical crack pattern is shown in Fig. 18 & 19 for control specimen and specimen G-3-10-Ag/2, respectively. For specimen GS-1.5-20-Ag, where GFRP strips were externally bonded, it was failed due to debonding of the strengthening strips, as shown in Fig. 20.

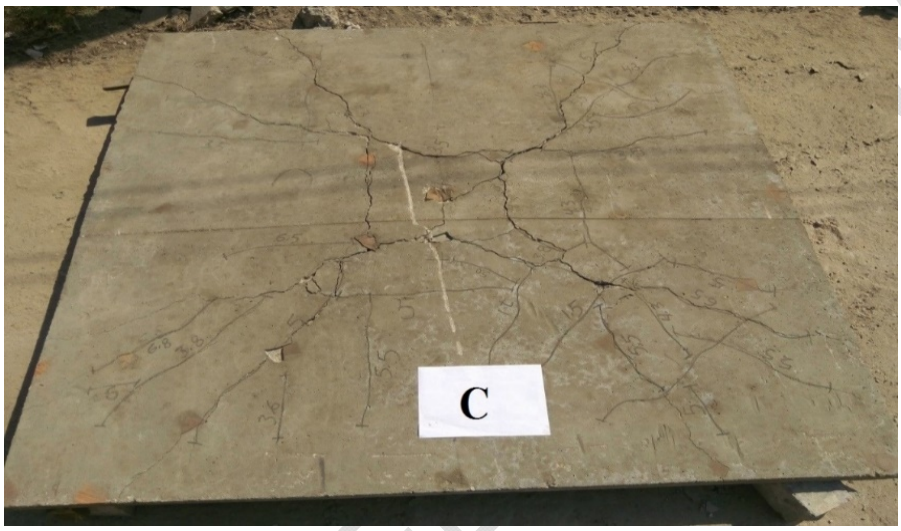

Fig. 18. Cracking pattern of specimen (C).

Fig. 19. Cracking pattern of specimen (G-3-10-Ag/2).

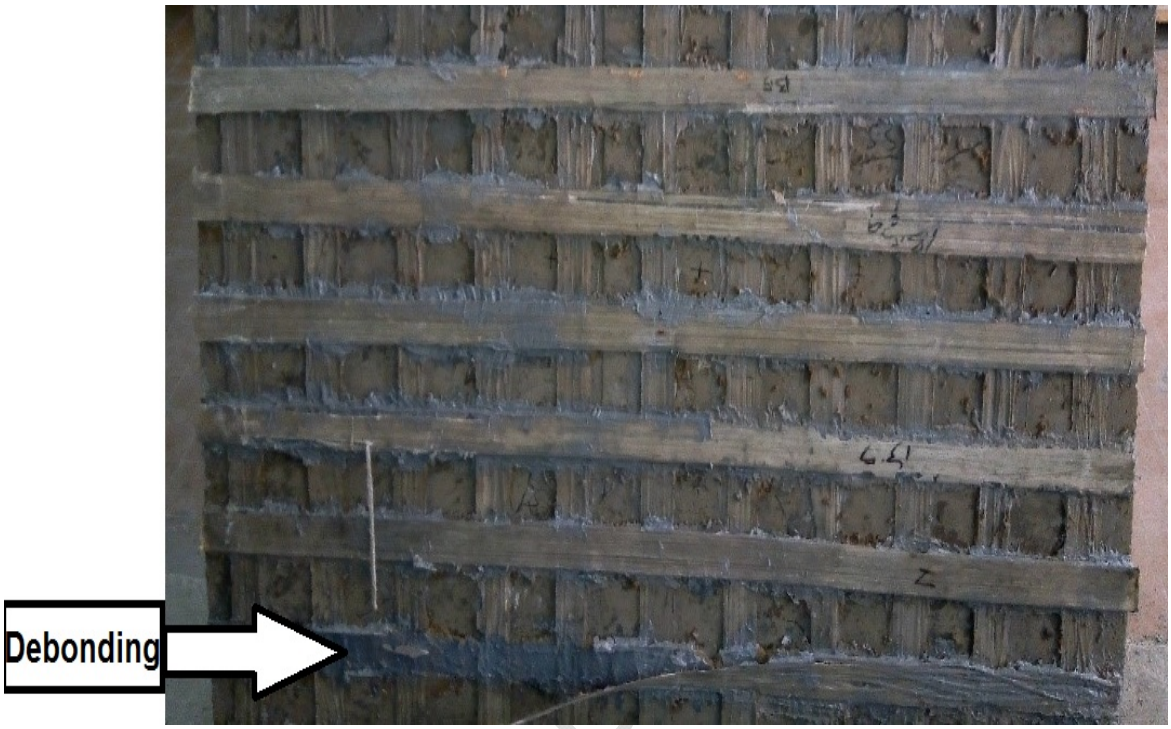

Fig. 20. Debonding shape for specimen (GS-1.5-20-Ag).

6. FINITE ELEMENT ANALYSIS

In this part, the tested specimens were simulated using the FEA program ANSYS (version 15). The numerical results of the simulated slabs were compared with the experimental results.

All the simulated models are simply-supported two way slabs subjected to four point load. The concrete and resin are modeled with a higher order 3-D element named SOLID65. LINK180 is used to define reinforcement steel and FRP bars while SOLID185 is used to define FRP sheets.

Many materials were used in modeling the specimens such as concrete, steel reinforcement, CFRP bars, GFRP bars, GFRP sheets and epoxy resin Sikadur® 330. The compressive stress-strain relationship of concrete is considered to be linear from zero to one-half the ultimate compressive strength, and the strain at the ultimate compressive strength ranges from 0.002 to 0.003. Reinforcement bars and shear connectors were modeled as a nonlinear and isotropic material. CFRP bars, GFRP bars and epoxy sikadur® 330 were modeled as linear isotropic material. GFRP strips were modeled by linear orthotropic material. Table. 6 presents the properties of the used material

Table. 6. The properties of the used materials.

Material	Compressive strength (MPa)	Tensile strength (MPa)	Poisson`s ratio	Modulas of elasticity (GPa)
Concrete	25	2.8	0.2	20
Steel bars	--	340	0.3	200
GFRP bars	--	1370	0.3	76
CFRP bars	--	1400	0.3	210
GFRP strips	--	2250	0.3	76

The experimental results obtained from testing of the tested specimens are compared with those obtained from the finite element modeling. The experimental and numerical results of load versus mid-span deflection are compared for each specimen, as shown in Figs. (21 to 31). The typical deformed shape of the finite element models obtained by ANSYS (version 15) is as shown in Fig. 32. Table. 7 presents a comparison between the numerical and experimental ultimate loads. It can be noticed that the ratio of the numerical ultimate load to experimental one ranged from 0.95 to 1.12. It can be observed that ANSYS almost predicts a higher ultimate load compared to the load observed during experiments.

Table. 7. Comparison of experimental and numerical results.

Specimen code	$P_{u, exp.}$	$P_{u, num.}$	$\frac{P_{u, num.}}{P_{u, exp.}}$
C	6.88	6.56	0.95
S-3-20-As	9.46	10.40	1.10
C-3-10-Ac/2	13.40	13.91	1.04
C-3-20-Ac	11.58	12.20	1.05
G-3-10-Ag/2	10.50	10.50	1.00
G-3-20-Ag	9.40	10.50	1.12
G-5-10-Ag/2	11.64	12.31	1.06
G-5-20-Ag	11.23	12.31	1.10
G-3-10-Ag	12.10	11.87	0.98
G-5-10-Ag	14.59	15.31	1.05
GS-1.5-20-Ag	11.74	11.60	0.99

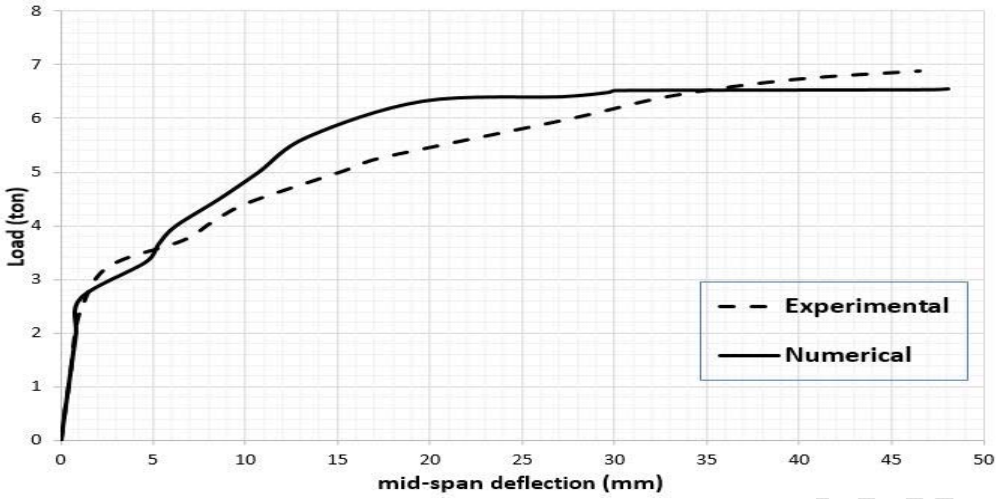

Fig. 21. Comparison between experimental & numerical load-deflection curves of tested specimen (C).

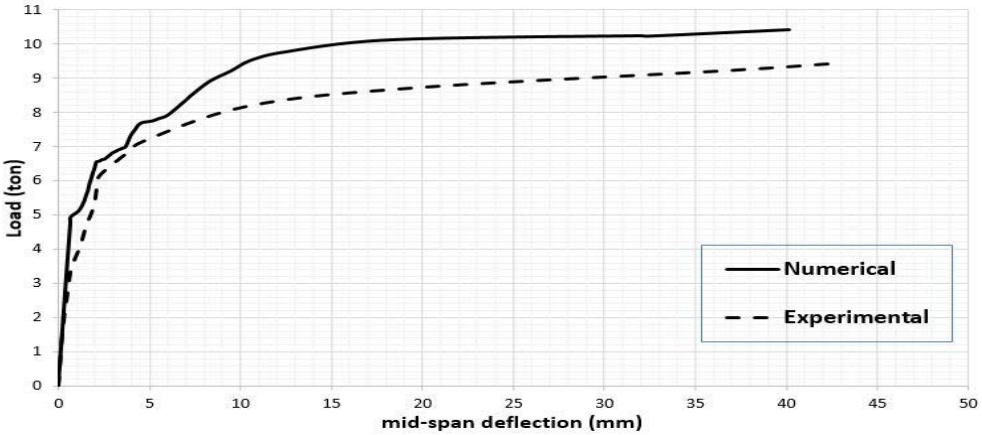

Fig. 22. Comparison between experimental & numerical load-deflection curves of tested specimen (S-3-20-As).

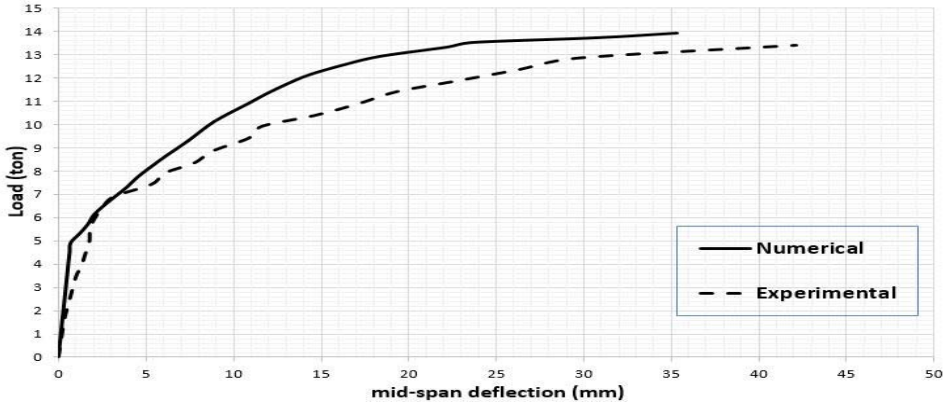

Fig. 23. Comparison between experimental & numerical load-deflection curves of tested specimen (C-3-10-Ac/2).

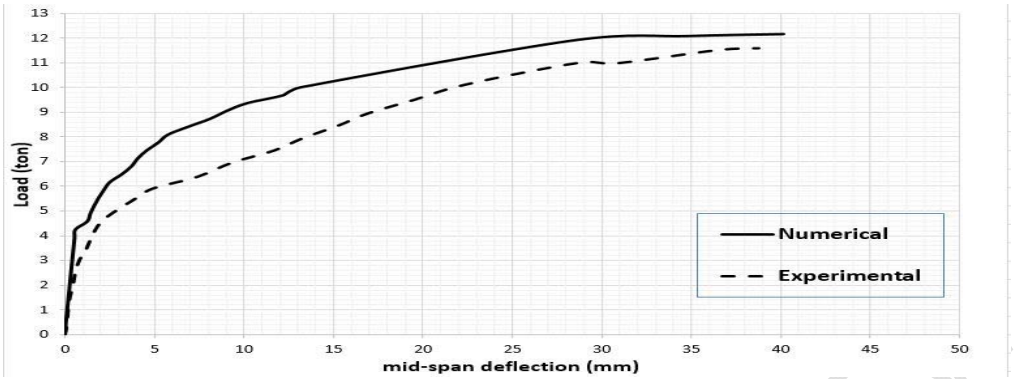

Fig. 24. Comparison between experimental & numerical load-deflection curves of tested specimen (C-3-20-Ac).

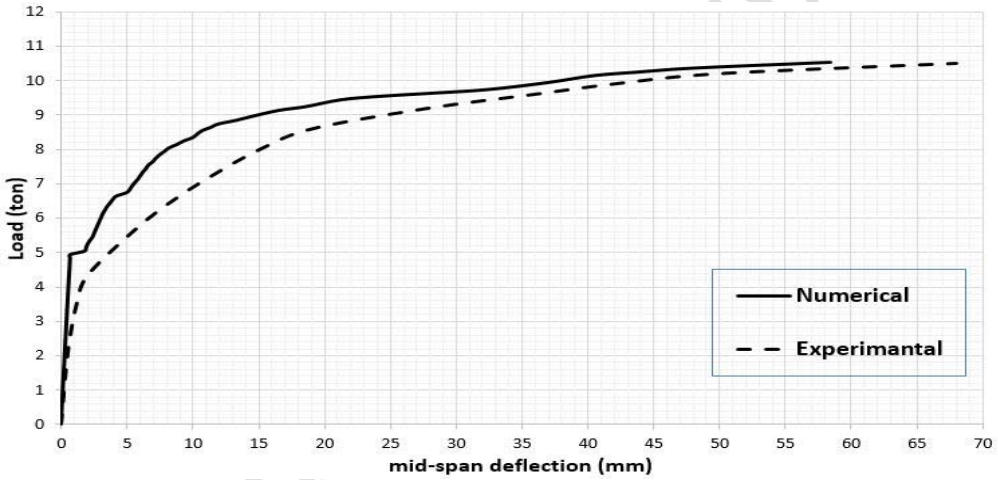

Fig. 25. Comparison between experimental & numerical load-deflection curves of tested specimen (G-3-10-Ag/2).

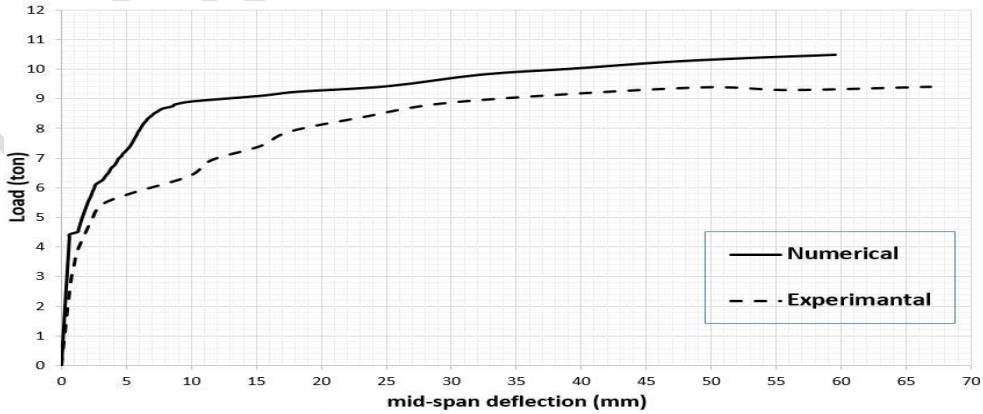

Fig. 26. Comparison between experimental & numerical load-deflection curves of tested specimen (G-3-20-Ag).

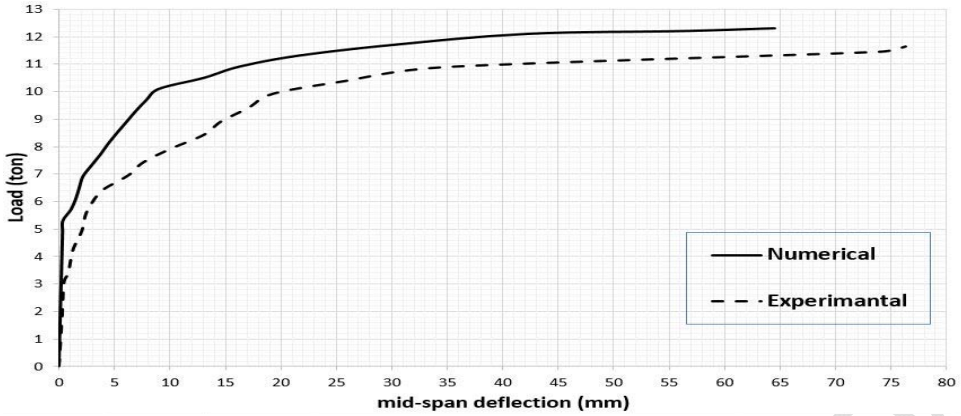

Fig. 27. Comparison between experimental & numerical load-deflection curves of tested specimen (G-5-10-Ag/2).

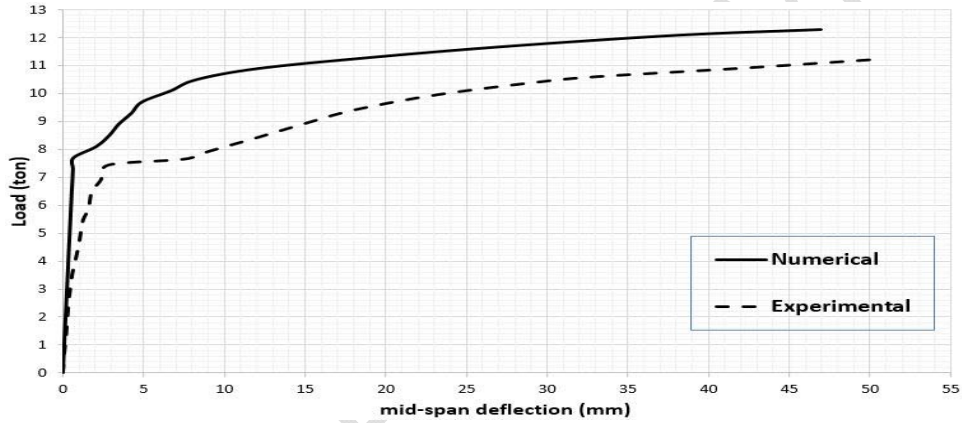

Fig. 28. Comparison between experimental & numerical load-deflection curves of tested specimen (G-5-20-Ag).

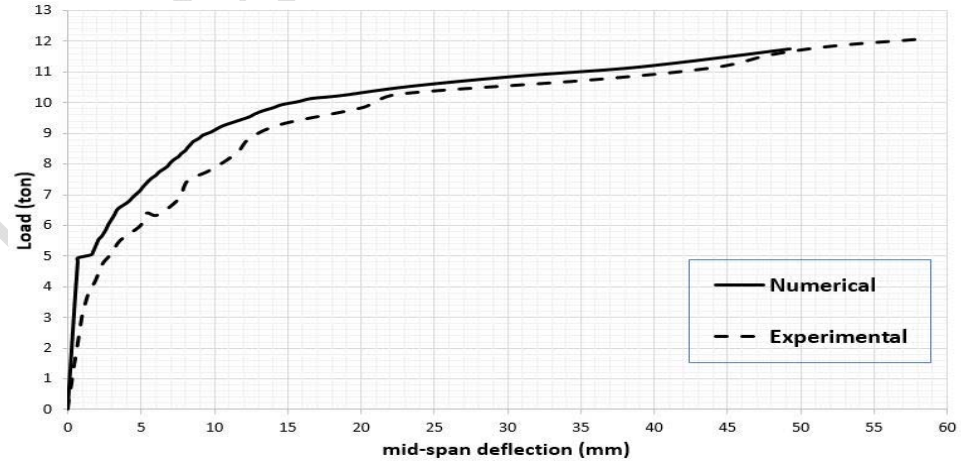

Fig. 29. Comparison between experimental & numerical load-deflection curves of tested specimen (G-3-10-Ag).

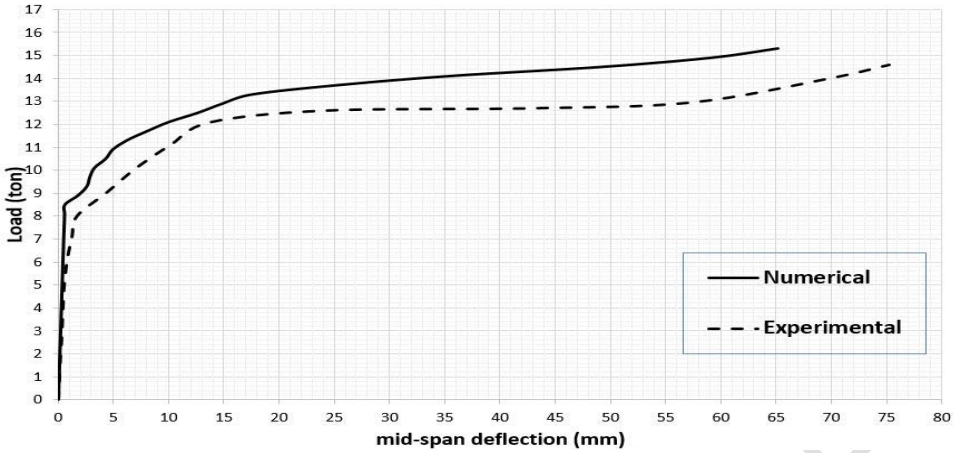

Fig. 30. Comparison between experimental & numerical load-deflection curves of tested specimen (G-5-10-Ag).

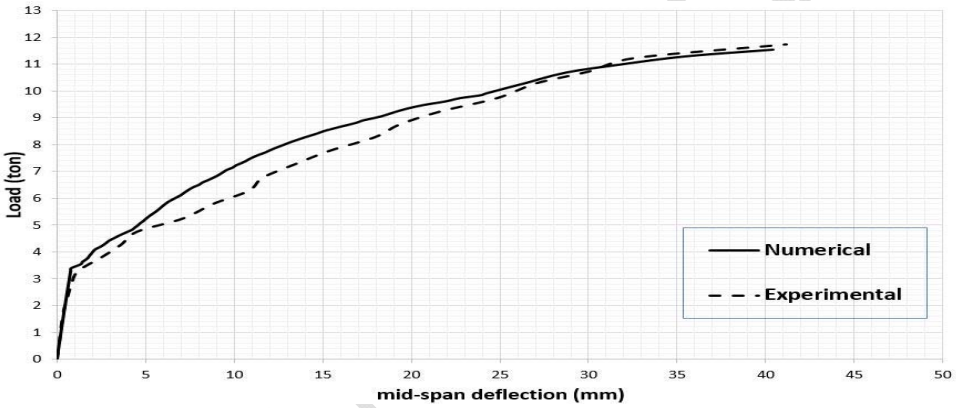

Fig. 31. Comparison between experimental & numerical load-deflection curves of tested specimen (GS-1.5-20-Ag).

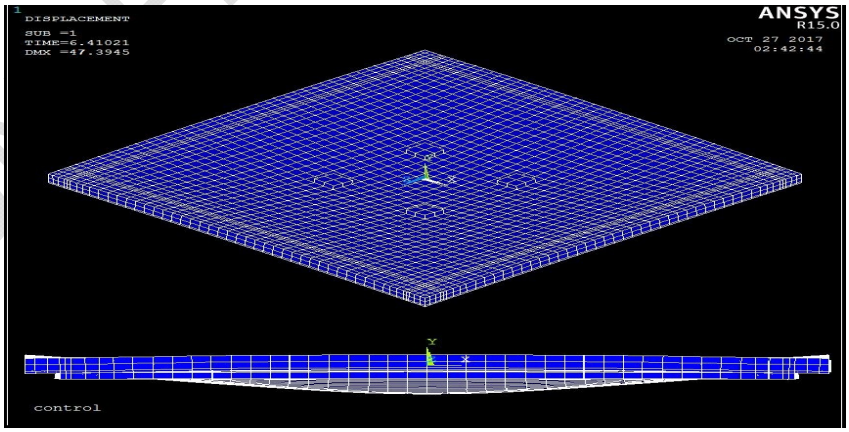

Fig. 32. Typical deformed shape of finite element model.

7. CONCLUSIONS

The main goal of the current research is examining the effect of adding R.C layer reinforced by FRP elements on the structural behavior of two-way R.C slabs in terms of strength and flexure. From the experimental and numerical results, the following conclusions could be drawn as below:-

- Strengthening systems were effective in improving the flexural strength of the tested specimens by a range from 37% to 112%, also, the deflections were reduced significally by a range from 75.3% to 97.5% compared to the control specimen at its ultimate load.
- All methods used for strengthening of slabs in this research were effective to restore and improve the structural performance in terms of flexural rigidity, ultimate stiffness (Ku), initial cracking load and the ultimate carrying capacity.
- All the used materials in this research led to increase the initial cracking load by 50% to 300% and the ultimate load capacity also increased by 37% to 112%.
- For the three types of strengthening material (reinforcement steel, carbon fiber and glass fiber); the specimens (S-3-20-As, C-3-20-Ac & G-3-20-Ag) achieved an increase in the initial cracking load by 100%, for the three specimens, and the ultimate capacity by 38%, 68% and 37%, respectively.
- For the strengthening layer thickness (30 & 50 mm); the specimens (G-3-10-Ag/2 & G-5-10-Ag/2) achieved an increase in the initial cracking load by 125% and 155%, respectively, and the ultimate capacity by 53% and 69%, respectively, also, the specimens (G-3-20-Ag & G-5-20-Ag) achieved an increase in the initial cracking load by 100% and 100%, respectively, and the ultimate capacity by 37% and 63%, respectively, also, the specimens (G-3-10-Ag & G-5-10-Ag) achieved an increase in the initial cracking load by 50% and 300%, respectively, and the ultimate capacity by 76% and 112%, respectively.
- For the spacing between reinforcement bars (100 & 200 mm); the specimens (G-3-10-Ag/2 & G-3-20-Ag) achieved an increase in the initial cracking load by 125% and 100%, respectively, and the ultimate capacity by 53% and 37%, respectively, also, the specimens (G-5-10-Ag/2 & G-5-20-Ag) achieved an increase in the initial cracking load by 155% and 100%, respectively, and the ultimate capacity by 69% and 63%, respectively, also, the specimens (C-3-10-Ac/2 & C-3-20-Ac) achieved an increase in the initial cracking load by 150% and 100%, respectively, and the ultimate capacity by 95% and 68%, respectively.

- For the reinforcement bars area (A & 2A); the specimens (G-3-10-Ag/2 & G-3-10-Ag) achieved an increase in the initial cracking load by 125% and 50%, respectively, and the ultimate capacity by 53% and 76%, respectively, also, the specimens (G-5-10-Ag/2 & G-5-10-Ag) achieved an increase in the initial cracking load by 155% and 300%, respectively, and the ultimate capacity by 69% and 112%, respectively.
- For the strengthening method (FRP bars & FRP strips); the specimens (G-3-20-Ag & GS-1.5-20-Ag) achieved an increase in the initial cracking load by 100% and 175%, respectively, and the ultimate capacity by 37% and 71%, respectively.
- For all the tested specimens, it was observed that the failure was flexural failure due to partial debonding between the strengthening layer and the original slab also, it was observed that the cracks began firstly at the slab tension side under four point load forming square line and with increasing the load, number and width of the cracks increase and begin to propagate in diagonal direction towards the slab edge.
- In general, the specimen (G-5-10-Ag) was the best one, which led to the highest ultimate capacity between the tested specimens. However the CFRP bars was the best material, which led to the highest improvement in the rigidity and ultimate capacity of the tested specimens.
- The numerical results used to predict the ultimate capacity of the tested specimens gave moderate conservative values, where the ratio of the numerical ultimate load and experimental one ranged between 0.95 to 1.12.

Authors' contributions

This work was carried out in collaboration between all authors. All authors read and approved the final manuscript.

REFERENCES

[1] Heiza K, Nabil A, Maleka N and Tayel M. (2014). State of the art review: Strengthening of reinforced concrete structures-different strengthening techniques. 16th international conference on nano technology in construction, Cairo, Egypt, March.

[2] Fernandes H, Lucio V and Ramos A (2017). Strengthening of RC slabs with reinforced concrete overlay on tensile face. Engineering structure.137, 540-550.

[3] Al-kubaisy, MA and Jumaat MZ (2000). Flexural behavior of reinforced concrete slabs with ferrocement tensions cover. J.Constr.Build. Mater., 14, 245-252.

[4] Ezzat, H F, Yousry BI, and Yasser SK (1996). Repairing reinforced concrete slabs using ferrocement laminates. 7th international colloquium on structural and geotechnical engineering, Cairo, Egypt, December.

[5] Calixto JM, Pires E F, Lima SA and Piancastelli EM (2003). Behavior of reinforced concrete slabs strengthened in flexure by concrete overlays. ACI Structural Journal 229, p.389-406.

[6] Michel L, Ferrier E, Agbossou A and Hamelin P (2009). Flexural stiffness modelling of R.C slab strengthened by externally bonded FRP. Composites: part B 40, p.758-765.

[7] Foret G and Limam O (2008). Experimental and numerical analysis of RC two-way slabs strengthened with NSM CFRP rods. J.Constr.Build. Mater., 22, 2025-2030.

[8] Foret, G, Limam O and Ehrlacher A (2003). RC two-way slabs strengthened with CFRP strips: experimental study and limit analysis approach. Composite structure. 60, 467-471.

[9] Tan KY, Tumialan G and Nanni A (2003). Evaluation of externally bonded CFRP system for the strengthening of RC slabs. Department of civil engineering, university of Missouri, Rolla, USA.

[10] Al-Rousan R, Issa M and Shabila H (2012). Performance of reinforced concrete slabs strengthened with different types and configuration of CFRP. Composites: part B 43, p.510-521.